LIMNOLOGY
and
OCEANOGRAPHY: METHODS

Limnol. Oceanogr.: Methods 12, 2014, 373–389

An assessment of the use of ocean gliders to undertake acoustic measurements of zooplankton: the distribution and density of Antarctic krill (*Euphausia superba*) in the Weddell Sea.

Damien Guihen[1], Sophie Fielding[1], Eugene J. Murphy[1], Karen J. Heywood[2], and Gwyn Griffiths[3]*
[1]British Antarctic Survey, Cambridge, United Kingdom
[2]University of East Anglia, Norwich, United Kingdom
[3]Autonomous Analytics, Southampton, United Kingdom

Abstract

A calibrated 120 kHz single-beam echo-sounder was integrated into an ocean glider and deployed in the Weddell Sea, Southern Ocean. The glider was deployed for two short periods in January 2012, in separate survey boxes on the continental shelf to the east of the Antarctic Peninsula, to assess the distribution of Antarctic krill (*Euphausia superba*). During the glider missions, a research vessel undertook acoustic transects using a calibrated, hull-mounted, multi-frequency echo-sounder. Net hauls were taken to validate acoustic targets and parameterize acoustic models. Krill targets were identified using a thresholded schools analysis technique (SHAPES), and acoustic data were converted to krill density using the stochastic distorted-wave Born approximation (SDWBA) target strength model. A sensitivity analysis of glider pitch and roll indicated that, if not taken into account, glider orientation can impact density estimates by up to 8-fold. Glider-based, echo-sounder–derived krill density profiles for the two survey boxes showed features coherent with ship-borne measurements, with peak densities in both boxes around a depth of 60 m. Monte Carlo simulation of glider subsampling of ship-borne data showed no significant difference from observed profiles. Simulated glider dives required at least an order of magnitude more time than the ship to similarly estimate the abundance of krill within the sample regions. These analyses highlight the need for suitable sampling strategies for glider-based observations and are our first steps toward using autonomous underwater vehicles for ecosystem assessment and long-term monitoring. With appropriate survey design, gliders can be used for estimating krill distribution and abundance.

Marine ecosystems are variable at a range of scales, from the small scales of processes associated with individual organisms to the large scales arising from climate forcing. Understanding the causes and consequences of ecosystem variability is an essential step toward the better interpretation of ecosystem function. Such understanding is pertinent to addressing the issues of Ecosystem Based Fisheries Management (Lubchenco et al. 1991; Constable 2001; Reid et al. 2010) and assessing the impact of climate and fisheries on marine populations. To observe and measure ecosystem variability, concurrent biological and physical oceanographic measurements are required at suitable temporal and spatial scales. This work has typically been undertaken from research vessels, which can provide comprehensive overviews, but are costly and, as a result, usually constrained to a limited, temporal, operating window. Consequently, alternative technologies, such as drifters, moorings, and Autonomous Underwater Vehicles (AUV), are increasingly being employed to provide cost-effective, extensive temporal, and/or spatial coverage (Brierley et al. 2003, 2006; Fernandes et al. 2003; Ullgren and White 2010).

The ability of sophisticated AUVs to assess zooplankton acoustically has been examined in order to make observations in challenging environments such as under ice (Griffiths et al. 2001). The ability of smaller, cheaper systems such as ocean gliders (Webb et al. 2001; Eriksen et al. 2001; Sherman et al. 2001) to undertake similar measurements is, however, at the limit of technological development. Ocean gliders are slow moving platforms that dive to depths of up to 1500 m, although deeper diving variants are currently under development (Osse and Eriksen 2007). Gliders are commanded remotely by pilots, and data are uploaded via radio or satellite links and new operating parameters downloaded when the glider returns to the surface (Eriksen et al. 2001). These gliders

*Corresponding author: E-mail: damaoi@bas.ac.uk

Acknowledgments

Full text appears at the end of the article.

DOI 10.4319/lom.2014.12.373

can make measurements over several months but can house only compact, low power (<1 W average power) sensors to enable these long mission durations. Sensors for measuring environmental parameters such as temperature, conductivity, chlorophyll, dissolved oxygen, and turbidity are now routinely mounted on gliders, thus contributing to unique observations of oceanographic biophysical interactions (Davis et al. 2008; Perry et al. 2008; Asper et al. 2011), physical and chemical oceanography (Johnson et al. 2009; Shulman et al. 2009; Queste et al. 2012). The ability of gliders to measure higher trophic levels, such as zooplankton and marine mammals, using active and passive acoustics is in development (Baumgartner & Fratantoni 2008; Dassatti et al. 2011; Klinck et al. 2012; Yahnker et al. 2012).

In this article, we assess the use of an echo-sounder, mounted on an ocean glider, to make quantitative measurements of acoustic backscatter from zooplankton. Our case study is an investigation of the abundance and distribution of *Euphausia superba* (Antarctic krill) measured concurrently from a Seaglider and from a research vessel. Antarctic krill is a central species in the Southern Ocean ecosystem and, with a circumpolar, post-larval annual production estimated to be 342–536 Mt yr^{-1}, one of the most abundant species on the planet (Atkinson et al. 2009). They are an important resource to many higher predators such as fish, seals, penguins (Croxall et al. 1985; Croxall et al. 1999), the subject of commercial fishing (Nicol and Endo 1999) and can have large inter and intra-annual variations in density and distribution influenced by local and global oceanography (Murphy et al. 2007; Atkinson et al. 2009; Reid et al. 2010). As a result Antarctic krill (hereafter krill) are a key subject of an international ecosystem/fisheries management system, CCAMLR (Commission for the Conservation of Antarctic Marine Living Resources). This management system has been informed by multi-national basin scale and national inter-annual assessments of krill distribution and abundance, undertaken using active acoustic methods (Watkins et al. 2004; Fielding et al. 2011; Reiss et al. 2008). Acoustic surveys of krill and fish density are typically performed from a surface vessel with hull-mounted, calibrated, multi-frequency echo-sounders. The following are some of the principal conditions that must be met for the collection of the acoustic data: (1) collection of time-stamped, depth-resolved, calibrated measurements of mean volume backscatter (dB re 1 m^{-1}) [a logarithmic scale]; (2) robust methodology for target identification of the key species in the acoustic data; (3) robust methodology for converting acoustic backscatter data to organism biomass (e.g., a validated target strength model); and (4) appropriate depth and spatial coverage of the survey area.

We address these four conditions, with particular reference to the integration of a low-powered echo-sounder into an ocean glider. We compare glider-derived estimates of krill density with concurrent, ship-borne measurements and undertake sensitivity analyses to inform on best practices.

Materials and procedures

The acoustic performance of an echo-sounder carried by an ocean glider was examined following two back-to-back cruises of the R.R.S. *James Clark Ross*, JR260b and JR255a. JR260b (26 Nov 2011 to 16 Jan 2012) undertook an acoustic assessment of krill distribution and abundance on the South Georgia shelf in the South Atlantic Ocean (Western Core Box, Fielding et al. in press) and provided an opportunity to calibrate the echo-sounders used during this study. JR255a (20 Jan 2012 to 3 Feb 2012) was a cruise to examine the use of gliders in Antarctic science (GENTOO project: Gliders: Excellent New Tools for Observing the Ocean). Acoustic transects using a hull-mounted multi-frequency echo-sounder, CTDs, and mid-water trawl net hauls were undertaken on the continental shelf to the east of the Antarctic Peninsula in the northwestern Weddell Sea (Fig. 1).

Ship-borne echo-sounder measurements

Mean volume backscatter (S_v, dB re 1 m^{-1}) data were collected throughout both cruises using a hull-mounted Simrad EK60 echo-sounder (38, 120, and 200 kHz). Standard-target echo-sounder calibrations (Foote et al. 1987) were conducted in Stromness Bay (54° 9.51 S, 36° 41.7 W) during JR260b and in the lee of a large iceberg (63° 8.82 S, 51° 44.8 W) during JR255a. Power settings were consistent between cruises, pulse duration was set for all frequencies to 1.024 ms and the interval was 1.5–2.5 s, depending on synchronization with other instruments. Acoustic data were processed in Myriax Echoview software version 4.80 as follows: relevant values for the speed of sound and absorption coefficients were derived from station CTD data and input; surface noise and false bottom echoes were identified and excluded from further analysis; interference spikes were corrected using a 3 × 3 matrix convolution algorithm to identify and remove cells within single pings having a difference greater than 40 dB from the surrounding cells; time-varied gain (TVG) amplified background noise was subtracted (Watkins and Brierley 1996).

For the purpose of comparing glider-derived acoustic data with ship-borne measurements, the EK60 data used in the comparison were selected solely from regions corresponding to the geographic extents of the glider deployments (Table 1, Fig. 1).

RMT8 sampling

Krill were sampled during JR255a using a mid-water trawl with a rectangular 8 m^2 mouth opening (RMT8, Roe and Shale 1979), comprising two opening and closing nets with a 4 mm mesh in their hind-section (Fig. 1). A total of 7 trawls were targeted on acoustic marks identified in the glider-deployment regions from the ship's real-time EK60 data display. Each trawl was comprised solely of Antarctic krill and up to 100 krill from each measured for length. Total length (TL, in mm) was measured from the anterior margin of the eye to the tip of the telson without the terminal spines, rounded down to the nearest mm (Morris et al. 1988). Length frequency distribution was

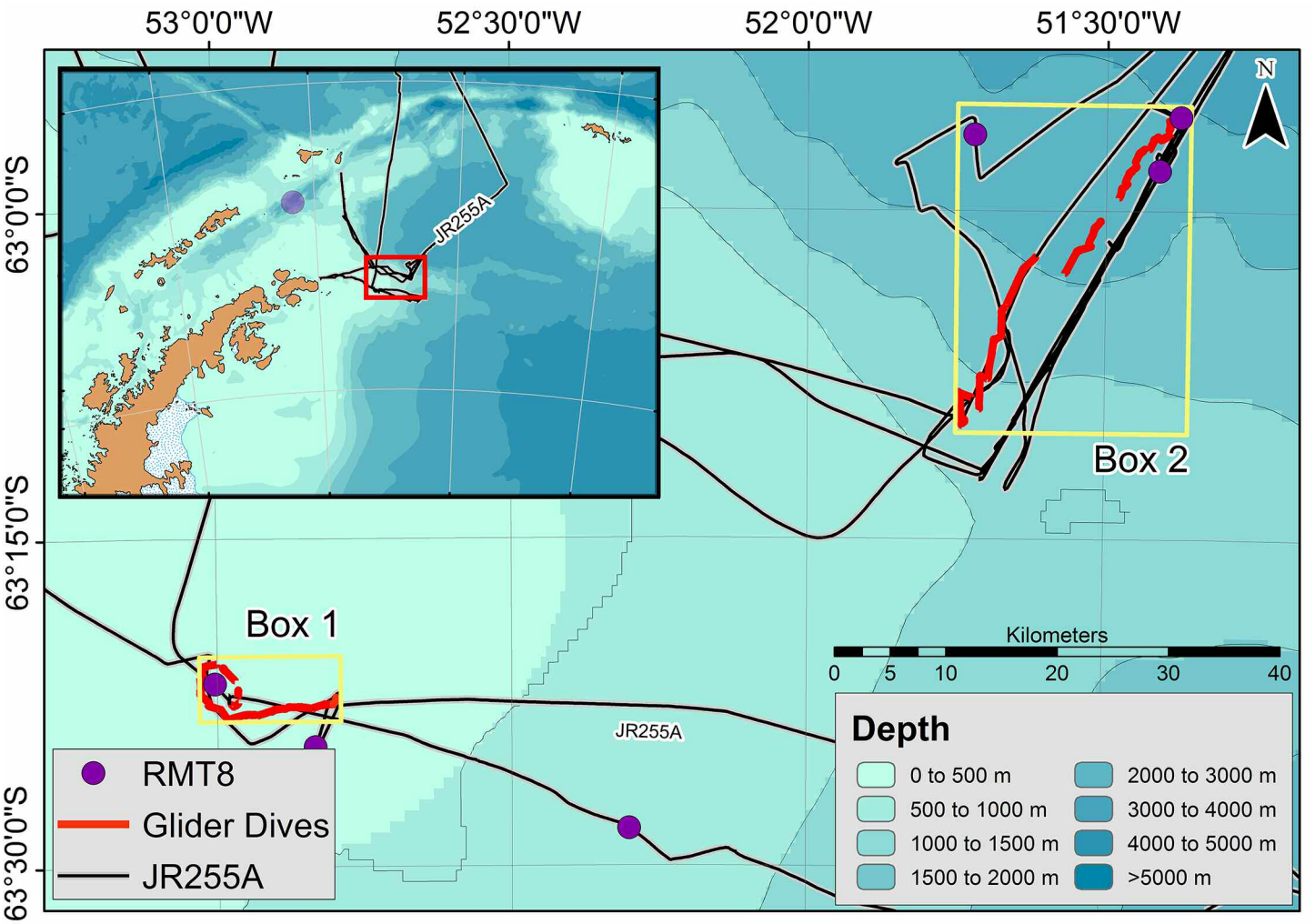

Fig. 1. Overview map of the glider deployments, RMT8 net hauls and ship's track, showing Boxes 1 and 2. The inset shows the location in the Weddell Sea.

Table 1. Geographic extents of Box 1 and Box 2, used for the comparison of ship-based EK60 and glider-based ES853 data.

Extent	West	East	North	South
Box 1	53° 57.0′ W	52° 15.0′ W	63° 35.4′ S	63° 36.6′ S
Box 2	51° 13.8′ W	51° 39.0′ W	62° 4.8′ S	63° 49.2′ S

based on 1 mm increments (n = 1386).

Glider-borne echo-sounder measurements

The echo-sounder

The acoustic performance of the echo sounder is clearly of paramount importance. However, to be deployed on a glider, an acoustic sensor also needs to be small, have low power consumption, and (ideally) be interoperable with the glider. The ES853 echo-sounder (hereafter ES853) was commissioned from Imagenex and is 3.5 inches (88.9 mm) tall with a diameter of 3.25 inches (82.55 mm), operates from a 24V DC power supply with a draw of 0.25 W, and communicates with the glider through a serial connection. The ES853 is a single-beam echo-sounder and has an operating frequency of 120 kHz, a pulse length of 100 μs, beam angle of 10°, range of 100 m, configurable gain of either 20 or 40 dB (only the 40 dB gain is considered here) and measures mean volume backscattering (S_v, dB re 1 m^{-1}) per range bin interval of 0.5 m. The ES853 can operate in three modes: real-time logging to a computer with a variable ping rate dependent on serial communication rate (typically ~ 2 Hz), self-logging with a ping rate of 1 Hz, or self-logging at a rate of 0.25 Hz ('glider mode'). The ES853 records a Range Bin

Value (RBV) at each bin interval, consisting of a 7-bit (i.e., allowing integers between 0 and 127) logarithmic value referenced to a 1-volt peak to peak signal, in the form 20 $\log_{10}$ (signal level/1 V peak to peak) such that 0 represents 1 V peak to peak and 120 represents 1 microvolt peak to peak (the values are negative, but stored as positive). RBV were converted to mean volume backscattering strength using an active version of the SONAR equation (Eq. 1) for distributed targets (Urick 1983).

$$S_v = RBV + 20log_{10}R + 2\alpha R - \left(RR + SL\right) - \left(10log_{10}\frac{c\tau}{2}\right) - \left(10log_{10}EBA\right) - C - g \quad (1)$$

where R is range (m), RBV is the recorded count (20$\log_{10}$[signal level/1V peak-peak]), RR is the transducer receiving response (dB re 1 V/μPa), and SL is the transducer source level (dB re 1 μPa at 1m) supplied by the manufacturer, α is the absorption coefficient (dB m^{-1}), c is sound velocity (m s^{-1}), τ is pulse length (s), EBA is the equivalent beam angle (steradians), *C* is a constant calculated during the calibration of the echosounder, and *g* is the gain (dB). The ES853 has a dynamic range of 120 dB and records signals as integer values, thus the resolution in signal strength is reduced compared with ship-based echo-sounders such as the EK60.

Calibration of the ES853 was performed in Stromness Bay, South Georgia during JR260b. An on-axis, standard-target sphere calibration (Foote et al. 1987) was performed with the ES853, using a 38.1 mm tungsten carbide sphere suspended from a small floating platform next to the ship. Calibrations were performed at a gain of 40 dB and at variable distances from the transducer face. Relevant values of speed of sound and sound absorption were derived from a CTD cast immediately before the calibration.

Glider deployment and motion

The ES853 was integrated into Seaglider SG546 (Fig. 2a) and was first deployed on 23 Jan 2012 at 63° 22.62′ S, 52° 58.62′ W, an on-shelf location with a water depth of 450 m. SG546 was piloted for 27 hours to a position 9 km away, having traveled a distance of 30 km, performing 11 dives (deepest: 405 m) with useable acoustic data (i.e., no logging errors). The second deployment was made on the 27 Jan at 62° 55.8′ S, 51° 21.78′ W, a location at the edge of the shelf with depth of 1200 m, increasing steeply to 2600 m during the course of the glider mission. The glider was piloted for 65 hours and recovered 32 km from its initial point, after traveling 59 km, performing 12 dives (deepest: 992 m) with useable acoustic data. Two dives from each box contained data corruption and were not included. The geographic extents of the two glider deployments are represented by two regions, Box 1 and Box 2, which we use for comparison with ship-based EK60 acoustic data collected during the glider deployments (Table 1, Fig. 1).

The ES853 was mounted in the ogive-type fairing, pointing

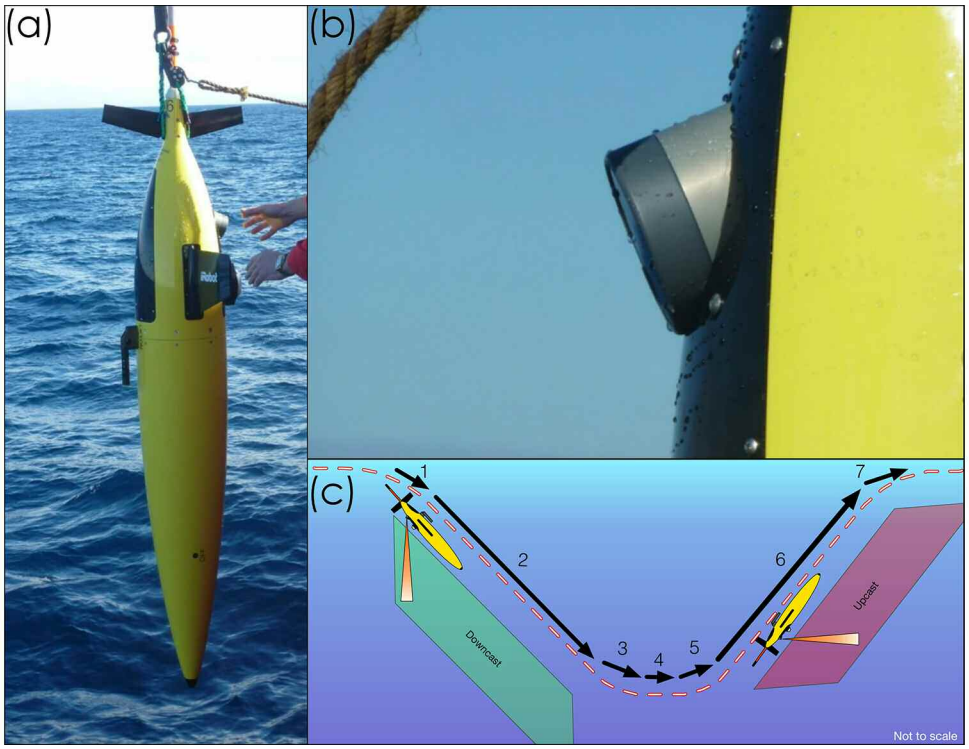

Fig. 2. (a) Photograph of the glider being deployed, (b) detail of the echo-sounder integrated into the fairing of the glider, and (c) diagram of echo-sounder orientation throughout a dive with numbered dive stages.

Table 2. 'Swarms analysis' parameters used to identify krill swarms by their morphological characteristics.

Parameter	EK60/ES853 Comparison	ES853 Sensitivity 1	ES853 Sensitivity 2
Minimum total school length (m)	15	3, 6, 12, 15, 24, 48, 96	15
Minimum total school height (m)	2	2	2
Minimum candidate length (m)	10	1.5	10
Minimum candidate height (m)	1	2	1
Maximum vertical linking distance (m)	5	2	5
Maximum horizontal linking distance (m)	15	3	15
S_v threshold (dB)	–70	–70	–68, –69, –70, –71, –72, –73, –74, –75

center along the short axis of the glider and 67.5° from the long axis, toward the nose, such that when the glider was in a typical downward glide of –22.5° with no roll, the echo-sounder pointed directly downwards, analogous with the downward-looking orientation of a ship's echo-sounder (Fig. 2b&c). The Seaglider uses changes in pitch and roll to maneuver, effected by shifting of the battery mass. To account for changing aspect, the orientation of the ES853 away from vertically down (both roll and pitch) was calculated as deviation (d) for each sample using a Pythagorean formula, where p is glider pitch and r is glider roll:

$$d = \sqrt{\left(p + 22.5\right)^2 + r^2} \quad (2)$$

Measurements of glider deviation were examined throughout the dive progression, which was divided into seven distinct stages identified by large changes in pitch; move from surface (stage 1), downward glide (stage 2), move to apogee (stage 3), apogee – horizontal motion only (stage 4, no data as new file made), move from apogee (stage 5), upward glide (stage 6), move to surface (stage 7) (Fig. 2c).

Glider acoustic data processing

The ES853 was operated in glider mode at a ping rate of 0.25 Hz, and data were recorded to internal memory. Transmission of the > 1 Mb acoustic files would have incurred significant Iridium satellite data transfer costs and greatly increased glider time at the surface, further subjecting the unit to the dangers of ice and surface currents. Raw echo intensity data were converted to S_v in MathWorks Matlab software using Eq. 1. Systemic interference, corresponding to individual saturated values, caused by an unrelated malfunctioning instrument also housed in the Seaglider fairing, were identified and replaced with NaN values. The location, depth, and orientation of each acoustic ping were calculated through the time-coordinated interpolation of the glider position and attitude data, with the glider navigation sampling at four times the rate of the ES853. Acoustic (S_v), position, and platform orientation (pitch, roll, and depth) data were then imported into Myriax Echoview software (version 4.80). A time-varied gain amplified background noise was subtracted (Watkins and Brierley 1996), the S_v data were corrected for the change in pointing direction of the transducer between transmission and reception caused by variations in glider pitch and roll with a maximum correction factor (k) of 5 (Dunford 2005) and the depth of the echo-sounder accounted for. Finally, data at ranges within 5 m of the sea surface, below the detected seabed and 1 m from the glider were removed to remove bubble noise and spurious echoes.

Krill Density estimation

A school detection algorithm was applied to the corrected S_v, from both the ES853 and EK60 data using the Myriax Echoview "School detection module," which employs a SHAPES (Shoal Analysis and Patch Estimation System) algorithm (Coetzee 2000). Due to different sampling resolutions between the ship-borne EK60 (2 s ping interval, typical survey speed of 10 knots, surface data) and glider-borne ES853 (4 s ping interval, typical speed of 0.75 knots, undulating data, reduced sensitivity), school (hereafter swarms) detection parameters could be different between instruments. To compare EK60 and ES853 krill density estimates, swarms were identified on 120 kHz data as a group of gridded acoustic values that met minimum criteria for S_v threshold, swarm length and height (Table 2), described by Tarling et al. (2009) for EK60 data. A –70 dB re 1 m^{-1} threshold was employed for both instruments, because it was defined by Lawson et al. (2008) to represent the minimum volume backscattering strength (of one krill per m^3 of water) for which a given acoustic measurement can be considered to be part of a krill aggregation.

At a typical horizontal velocity of 0.75 knots and a ping interval of 4 s, the minimum horizontal resolution of the glider-borne ES853 data (1.5 m) is a factor of 5 smaller than that of the EK60 data (7.5 m). As a result, the glider data can be used to detect smaller krill swarms. A sensitivity analysis on the minimum swarm length was undertaken, using a minimum total swarm length of 3 m (double the minimum horizontal resolution) and doubling it until no swarms were detected. By only recording integer values of S_v per cell, the ES853 has a lower S_v resolution than the EK60. A sensitivity analysis on the S_v threshold value used for swarm detection was performed by undertaking the swarms analysis at different acoustic thresholds (–68 to –75 dB in steps of 1 dB).

S_v data attributed to krill were integrated to generate Area Scattering Coefficient (s_a, $m^2\ m^{-2}$). S_v was integrated from the sea surface to the bottom of the glider profile with a constant integration cell height of 5 m, (or to 2 m above the seabed) and at a cell width of 15 m. Cell integration values of s_a were converted to krill density (g m^{-2}) as follows. The krill length frequency data were used to derive weighted mean backscattering cross-sectional areas (σ_{bs}) on a per animal basis using the validated physics-based target strength (TS) model (SDWBA), parameterized with literature values of density and speed of sound contrasts given for South Atlantic krill (Demer and Conti 2005) and a fixed krill orientation of –20° (mean) and 28° (standard deviation) (hereafter N[–20,28]), as adopted by the Commission for the Conservation of Antarctic Marine Living Resources (CCAMLR) (SC-CCAMLR 2010).

$$\sigma_{bs} = 10^{TS/10} \quad (m^2\ krill^{-1}) \tag{3}$$

The krill length frequency data (TL, mm) were also used to calculate weighted-mean wet masses per animal (W, g $krill^{-1}$) using the mass-to-length relationship calculated for the Scotia Sea in 2000 (Hewitt et al. 2004):

$$W = 2.236 \times 10^{-6} \times TL^{3.314} \quad (g\ wet\ mass\ krill^{-1}) \tag{4}$$

Density (b, g wet mass m^{-2}) was calculated by multiplying the 120 kHz s_a attributed to krill by a weighted mean mass W, divided by a weighted σ_{bs} (Reiss et al. 2008):

$$b = s_a \times [\Sigma f_i \times W(TL_i)/\Sigma f_i \times \sigma_{bs}(TL_i)/1 \times 10^{-3}] \quad (g\ wet\ mass\ m^{-2}) \tag{5}$$

Assessment

ES853 sensitivity and calibration

The calibration target was suspended at 16, 29.5, 39, 51, 62.5, and 70 m below the ES853, and data recorded at 40 dB nominal gain setting (39.9 dB for the ES853 unit used). Because the ES853 is a single beam echo-sounder, it gives no information on the lateral position of the target within the beam. Therefore the maximum signal received (RBV) from the range bin in which the calibration target was suspended was assumed to be the "on-axis" value. The ES853 signal was found to saturate at an RBV of –23 dB (S_v of –43dB). For the target sphere used during calibration (38.1mm tungsten carbide), saturation would therefore occur at ranges less than 24 m (Fig. 3a). Consequently, the first calibration bin at 16 m was not useable, with the theoretical RBV of the target at this range being approximately 7 dB greater than the saturation threshold of the ES853. The theoretical and actual values of RBV of the target for the four remaining samples were within 1 dB of each other. Actual RBV values were less than theoretical at 29.5 m and higher than the theoretical below 39 m, indicating that the TVG gain function did not quite conform to the standard 20log$R$, and further work is required to measure the signal pro-

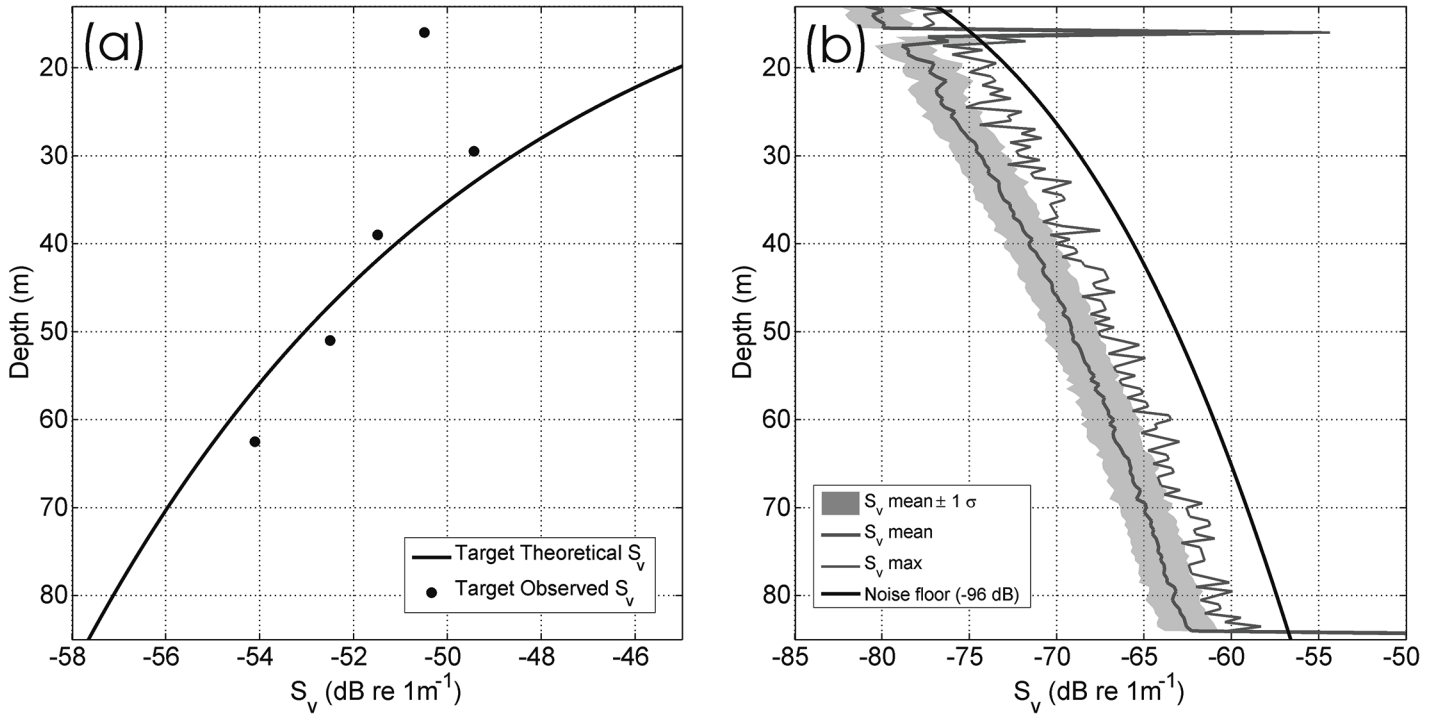

Fig. 3. (a) Theoretical and observed backscatter of the acoustic target, (b) mean and maximum profiles of backscatter with the target at 16 m and –96 dB noise floor of the echo-sounder during calibration at Stromness, South Georgia.

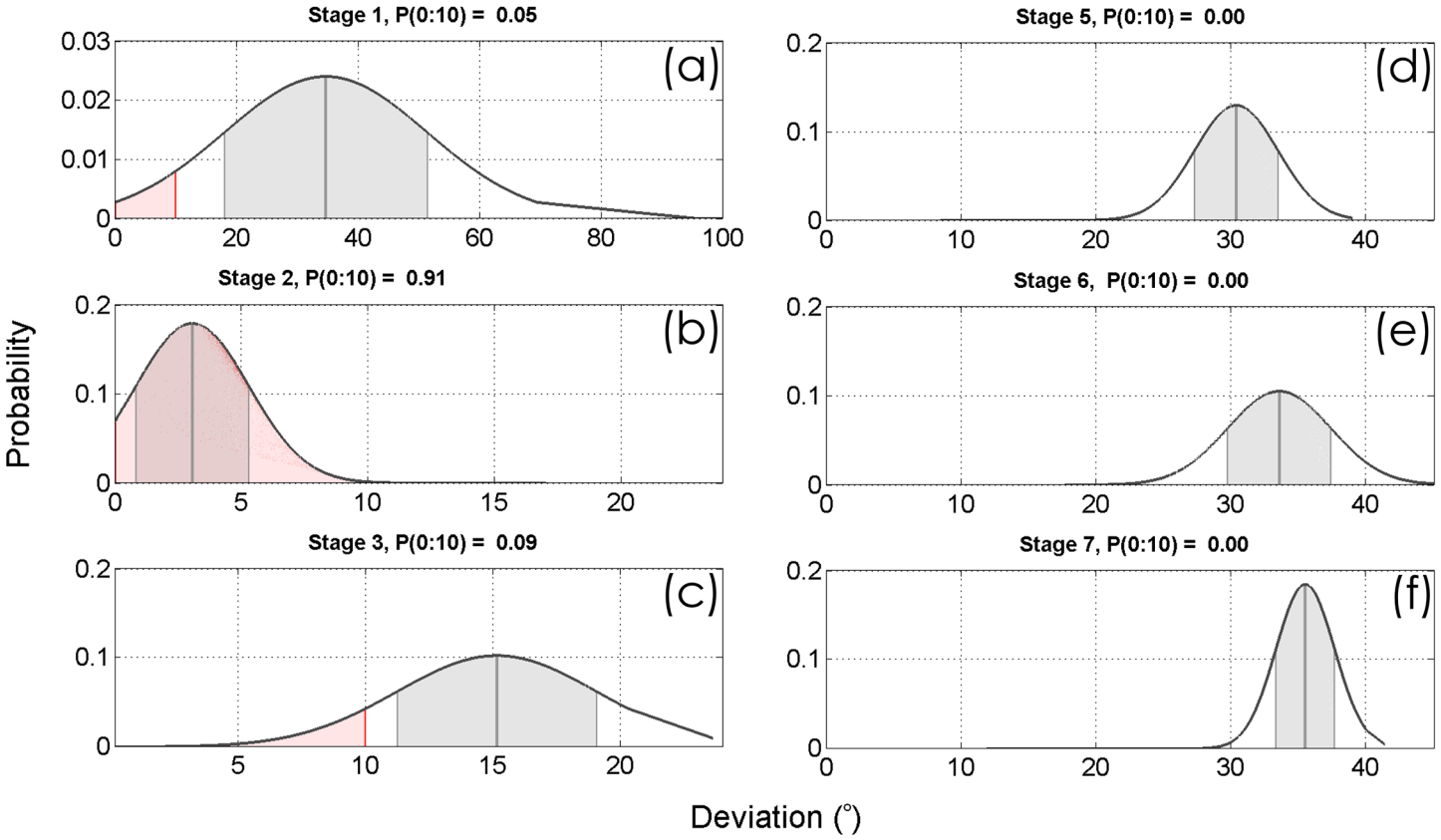

Fig. 4. Normal probability distribution functions calculated from raw data of echo-sounder deviation from vertical for (a) stage 1, (b) stage 2, (c) stage 3, (d) stage 5, (e) stage 6, and (f) stage 7. The mean is identified with a gray vertical line and 68% of the distribution (mean ± 1σ) is shaded in gray. The selected 0°-10° limit for this analysis is shaded in pink and the amount of data this represents within each stage is given.

cessing of the ES853 to reduce uncertainty of the S_v estimate. The ES853 was unable to detect the calibration sphere above background noise at a range of 70 m, which would have a theoretical S_v of –56.0 dB. Since the manufacturer-stated noise floor of the echo-sounder is –96 dB (re 1 V_{RMS}), any signal above –59 dB at a range of 70 m should be detectable. Given the challenge of locating a 38.1 mm sphere in the center of the single beam at a distance of 70 m, it is likely that the sphere was not within the center of the beam at this depth. Measurements of S_v through the water column, while the sphere was at 16 m, show that actual noise floor of the echo-sounder is –97 dB, close to the manufacturers estimate.

Glider orientation and impact on TS estimation

The efficiency with which an animal scatters sound is a function of acoustic frequency, the animal's size, shape, orientation, and material properties (Medwin and Clay 1998). In the case of Antarctic krill, whose shape is typically approximated by a rough, bent, tapered cylinder, empirical observation and modeled predictions of krill acoustic target strength indicate a high degree of directional sensitivity (McGehee et al. 1998). Ship-based acoustic surveys typically use downward-facing echo-sounders and estimate animal biomass using target strength models that assume an animal orientation with reference to that echo-sounder aspect. An underwater glider (Seaglider), bearing an echo-sounder, uses pitch (and roll) to move down or up (left or right), changing the incident angle of the acoustic signal to the animal target throughout the dive.

We assessed the orientation deviation (from vertical) of the echo-sounder mounted on the glider during different stages of the dive (Fig. 4). Transitional move stages (1, 3, 5, and 7) were periods where a significant proportion (>90%) of acoustic data were collected with the echo-sounder orientation deviating by > 10° from vertical. The upward glide stage (6) had a mean deviation of 35°, related to the significant change in pitch as the glider flies upwards. The movement toward a horizontal aspect of acoustic incidence introduces an additional complexity of heading (head on, side on, tail on) to TS estimation that requires further consideration. The downward glide stage (2) had > 90% of the collected acoustic data within 10° deviation from vertical. The Antarctic krill SDWBA target strength model is typically parameterized with a normal krill orientation distribution of N[–20°, 28°] (SC-CCAMLR 2010; Fielding et al. 2011). A total deviation of 10°

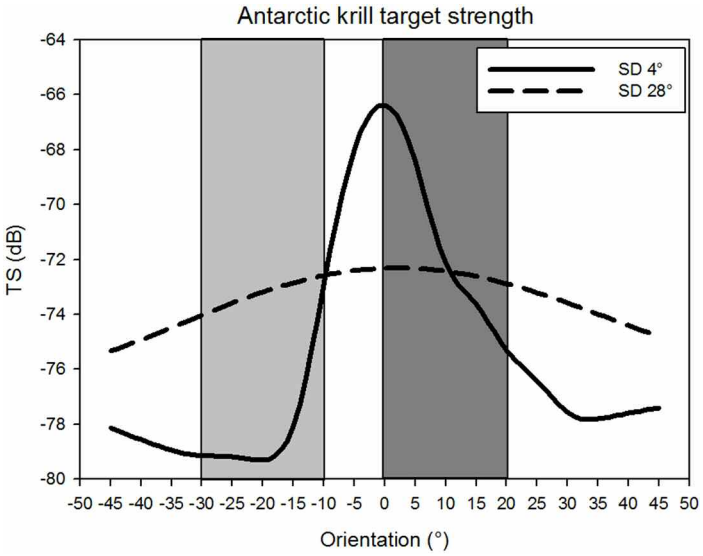

Fig. 5. The target strength (TS in dB) of a krill (32.55 mm) versus mean angle of acoustic incidence. The dashed line represents the CCAMLR 2010 estimated orientation distribution (N[–20°,28°]); the solid line represents a more constrained distribution of N[11°,4°] from Conti and Demer (2006). Light gray shaded area represent the 10° deviation allowed N[–20°,28], dark gray represents the 10° deviation around N[11°,4°]. An incident angle of 0° corresponds to a dorsal aspect.

(around a mean of –20°, with a standard deviation of 28°) would result in a change in TS of a 35 mm krill of 1.5 dB. However, if the standard deviation decreases around a mean (i.e., the krill are all orientated in the same direction – an N[11°,4°] as determined by Conti and Demer 2006), the variation in orientation of instrument of small amounts can result in more than an order of magnitude greater variation in TS at 8.9 dB (Fig. 5).

For the purpose of this study, and comparison with shipborne measurements, we selected acoustic data from the ES853 where the deviation from a downward aspect was < 10°, therefore only considering the down-glide data (stages 1-3). After application of the deviation threshold, the remaining data constituted 42% of the original acoustic dataset in both boxes. This value is highly dependent on the mission profile. Data were disproportionately excluded from the shallower dives, where surface and inflexion at maximum depth maneuvers constitute a much larger fraction of the dive. A longer mission with a greater proportion of trimmed, deeper dives should therefore expect a larger percentage of below deviation threshold data. Seaglider pilots can choose to make guidance and control maneuvers less frequently, or not at all, during dive stage 2. This would mean that the glider would be less able to navigate in a straight line toward a waypoint in strong currents, but the advantage would be better echo sounder data. Alternatively, a glider employing a rudder rather than a rolling center of mass would result in a greater proportion of usable downcast data, according to our criteria.

Estimation of krill density

The vertical distribution of krill

The detection of krill targets was undertaken on geo-referenced and calibrated arrays of S_v (Fig. 6). This was not a systematic survey of the boxes, thus comparisons between instruments are based on relative sampling effort in the same area and time. The EK60-derived mean, depth-integrated (to 400 m) density of krill along the transects in Box 1 (247.4 g m^{-2}) was three times that of Box 2 (81.8 g m^{-2}). The ES853 data showed an 8-fold difference in mean, depth-integrated (400 m) krill density between transects in Box 1 (162.0 g m^{-2}) and in Box 2 (20.1 g m^{-2}), with 35% and 75% less krill density in transects in Box 1 and 2, respectively, than that measured by the EK60 (Table 3).

The mean density profiles derived from both instruments show similar structures between instruments within the vertical distribution of krill, but highlight the different quantities of krill found in each box. In Box 1 both instruments show krill confined to the upper 150 m (Fig. 7a), with a peak density of 30.9 g m^{-2} (EK60) around 60 m. In addition, large and coherent standard deviations of up to 100 g m^{-2} were observed; over three times the maximum mean densities. The krill density profiles from Box 2 show krill constrained within the top 250 m of the water column, although most within the top 150 m. Maximum mean krill densities (7.4 g m^{-2}) were half to a quarter of those observed in Box 1. The large standard deviations relative to the low mean krill density estimated from the EK60 and ES853 data suggest there were a small number of swarms within the survey box. Whilst appearing similar in distribution, there are clearly differences between the krill density estimates from the EK60 and ES853. To account for these differences, we examined the sensitivity of the krill density estimate with respect to target identification, sensor sensitivity, and sampling strategy.

Sensitivity analysis of krill detection parameters and swath width

The distribution of krill is known to be patchy, with mean densities influenced by a small number of dense swarms (Fielding et al. 2012). Therefore, it is important to account for differences in the abilities of the EK60 and ES853 to detect krill swarms. As a consequence of the slower horizontal speed of the glider platform, the horizontal inter-ping distance of the ES853 acoustic data (1.5 m) is considerably shorter than that of the EK60 (7.5 m) when collecting data at typical survey speeds (e.g., 10 knots). As a result, in this setup, the ES853 is capable of resolving smaller krill swarms than the EK60 data at typical survey speeds (minimum 2 pings required). The effect of different swarm horizontal length detection limits within the SHAPES analysis showed that the estimate of krill density was not significantly affected by the minimum horizontal detection length varying between 3 and 15 m, with a difference of 3.3% of the integrated mean density in Box 1 and 1.9% in Box 2. However, a minimum detectable swarm length larger than 15 m strongly influenced the density of krill esti-

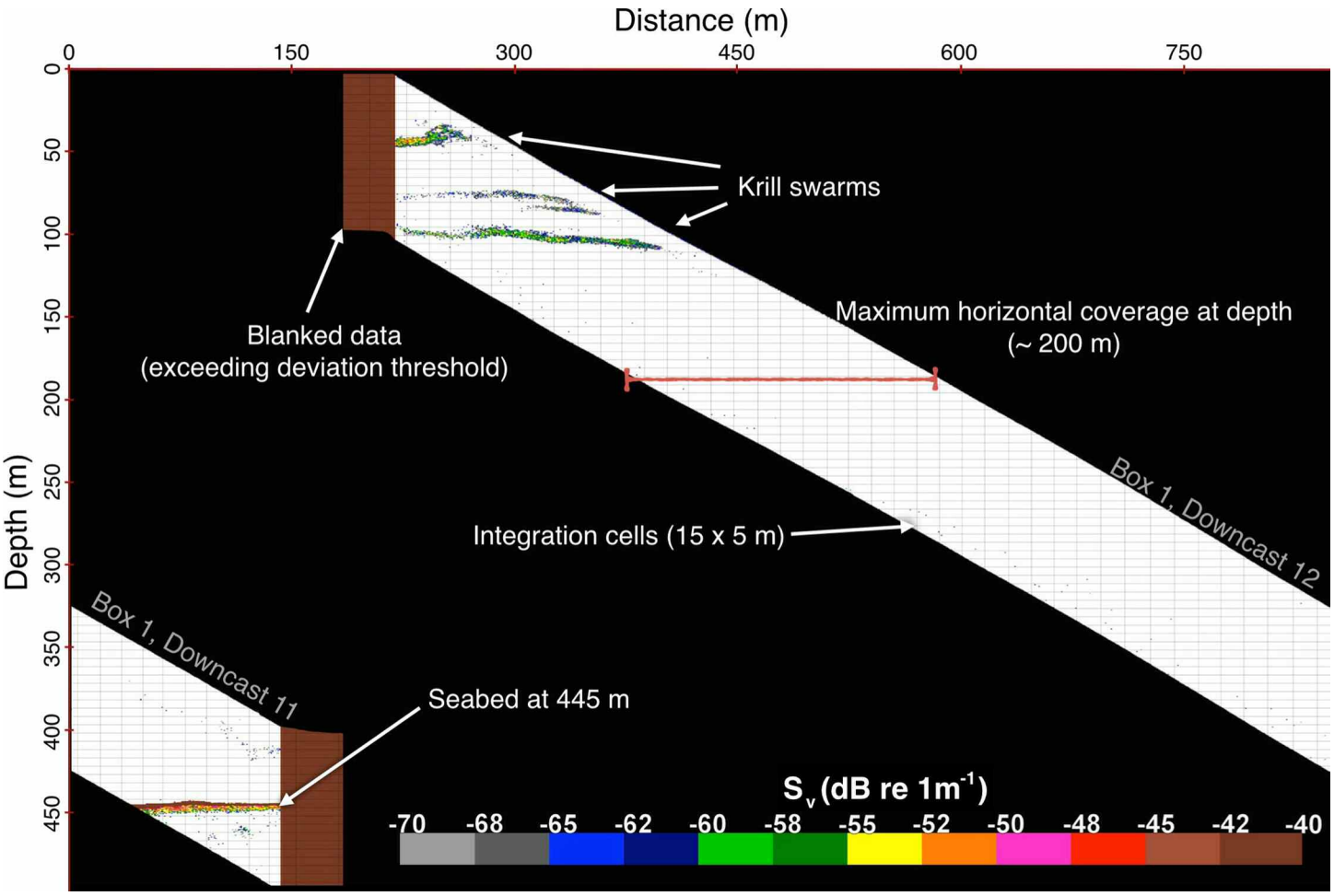

Fig. 6. Example of georeferenced and depth-corrected glider-derived acoustic downcast data, showing krill swarms, seabed, blanked data, and undulating coverage.

Table 3. Integrated krill density mean profile totals (g m^{-2}) for both instruments and boxes.

	EK60–JCR	ES853–Glider
Box 1	247.4	162.0
Box 2	81.8	20.1

mated, with 12% less krill in Box 1 and 53% in Box 2 using a 24 m minimum swarm length (Fig. 8a).

The impact of the signal to noise ratio on krill swarm delineation was examined by undertaking the swarms analysis at different thresholds. Because of the –96 dB noise floor, targets of –70 dB (approximately 1 krill per m^3 of water) are only detectable (i.e., have a signal to noise ratio > 1) within 45 m of the transducer (Fig. 3b). Lowering the threshold to –75 dB would restrict the range of the ES853 to 28 m. Only very slight increases in krill mean density (<1% at most) were observed by decreasing the detection threshold from –70 dB to –75 dB. Increasing the threshold to –68 dB was seen to lower krill density estimates by up to 0.25 g m^{-2} (1.25% max of mean density profile) in Box 1 (Fig. 8b), but over 1.6 g m^{-2} (40% max of mean density profile) in Box 2 (Fig. 8c). Because krill density estimates were not substantially greater using a lower threshold, it suggests that sensor sensitivity is unlikely to cause the large differences observed in the estimates of krill density between the EK60 and ES853 with the parameters used.

The ship-borne EK60 provides acoustic data continuously along the cruise track, from the surface to approximately 400 m water depth (at 120 kHz). The glider-borne ES853 samples acoustic data from an along-track length at any specific depth that is a function of its undulating dive profile and echosounder range. During glider reorientation stages, at the surface and bottom of the dive (1 and 3), this horizontal along-track length at any specific depth can be quite short (<100 m), whereas during the downcast glide stage (2), it is approximately 200 m wide. This results in orders of magnitude difference in sampling effort (i.e., area ensonified over time) between platforms and with depth (Fig. 7c).

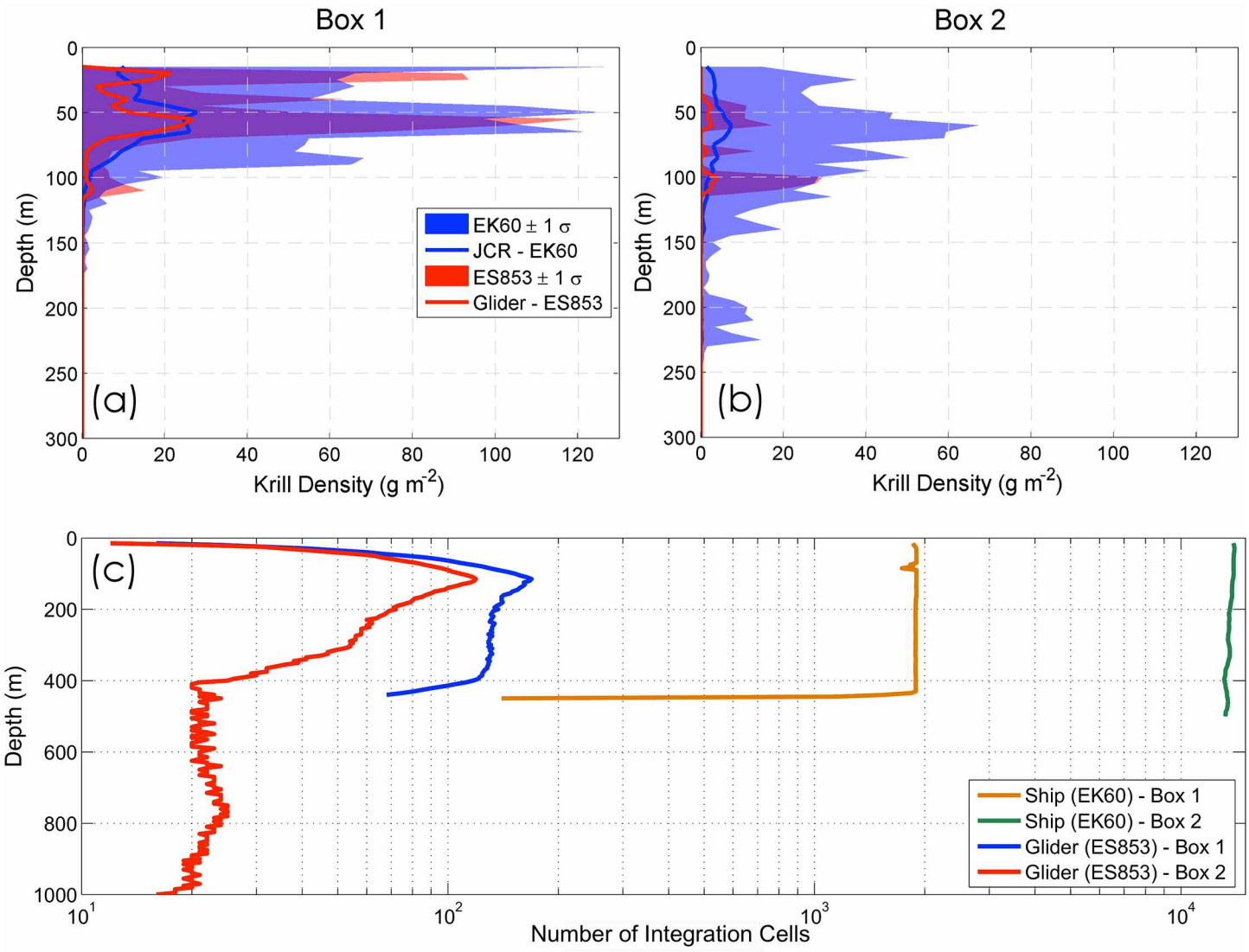

Fig. 7. Comparison of observed ship and glider-derived krill density profiles from (a) Box 1 and (b) Box 2. The number of integration cells by depth for both instruments and boxes is shown (c).

Glider acoustic horizontal sampling effort is greatest in both boxes between 110 and 120 m, increasing to, and decreasing from that point. Sampling effort is low in the upper 20 m for both boxes, at fewer than 20 integration cells (a cumulative distance of 300 m) across all dives. Similarly, dives to depths greater than 400 m made up a small portion of all dives in Box 2, thus the sampling effort is between 20 and 25 integration cells per depth. There is no sampling effort in either box for the EK60 below 500 m as the instrument lacks the range to penetrate the water-column beyond that depth. In addition, because an echo-sounder has a conical beam, the volume of water ensonified increases with depth. Therefore a ship-borne echo-sounder loses resolution with depth, whereas a glider's undulating profile ensures the sampling resolution as a function of beam width is consistent across all depths. This highlights the potential for glider-borne acoustics to make observations beyond the depth-range of hull-mounted instruments for examining the abundance of Antarctic krill distributions that have been identified in deep layers or near the seabed (Schmidt et al. 2011) or defining smaller krill swarms at depth.

The number of 15 m integration cells in the EK60 data are large (1898 cells in Box 1 and 14101 cells in Box 2) and constant with depth (Fig. 7c), varying only with the exclusion of data below the seabed (Box 1). The sampling effort of the glider is two orders of magnitude less and varies greatly with depth, up to 6-fold, in the case of Box 2. The poorer correspondence between the profiles in Box 2 than in Box 1 may be a consequence of these differences in sampling effort.

Sensitivity analysis of sampling effort

A Monte Carlo simulation (20,000 iterations of dive mission [11 dives in Box 1 and 12 dives in Box 2], with no replacement)

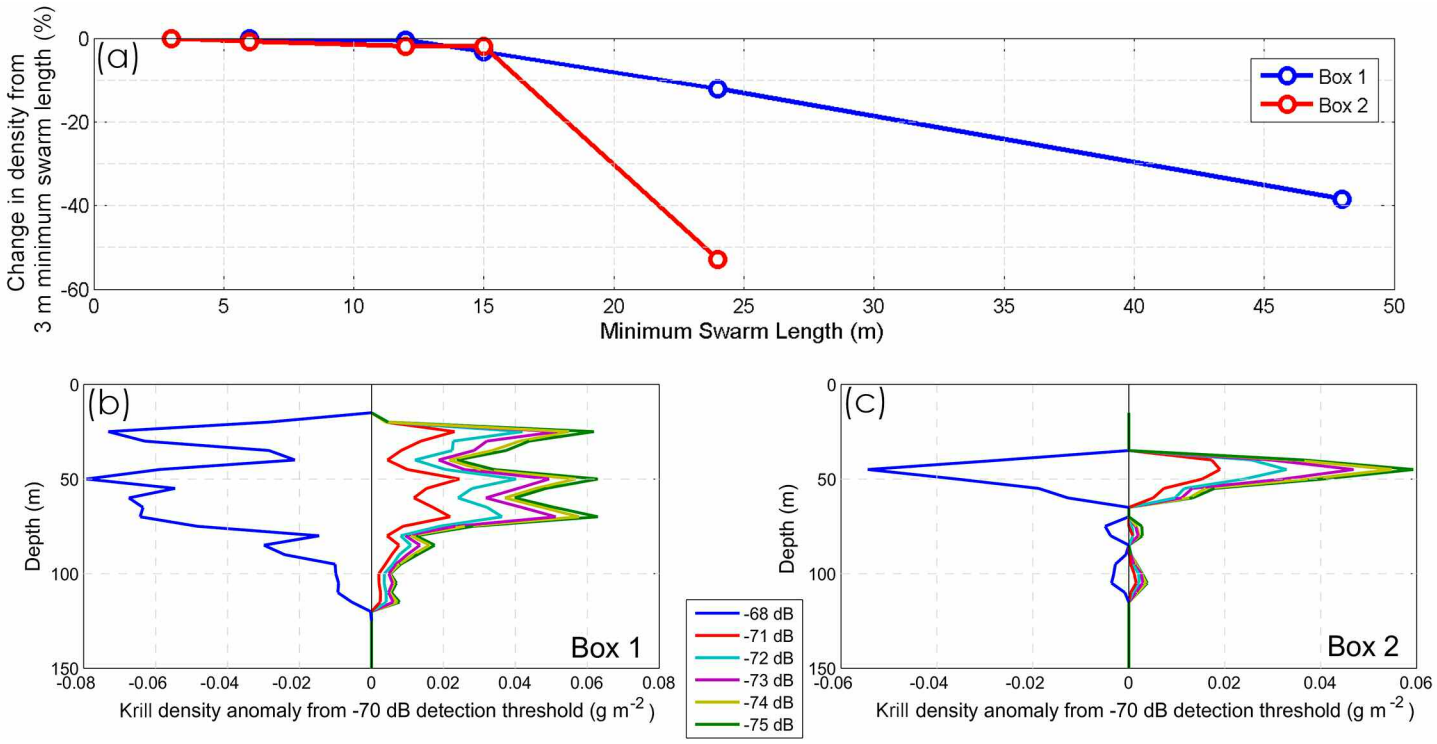

Fig. 8. (a) The difference in krill density (%) estimated using different minimum swarm candidate lengths from that calculated using a minimum swarm candidate length of 3 m for Box 1 (blue) and Box 2 (red). The difference in krill density (gm^{-2}) estimated with depth at different threshold levels for (b) Box 1 and (c) Box 2.

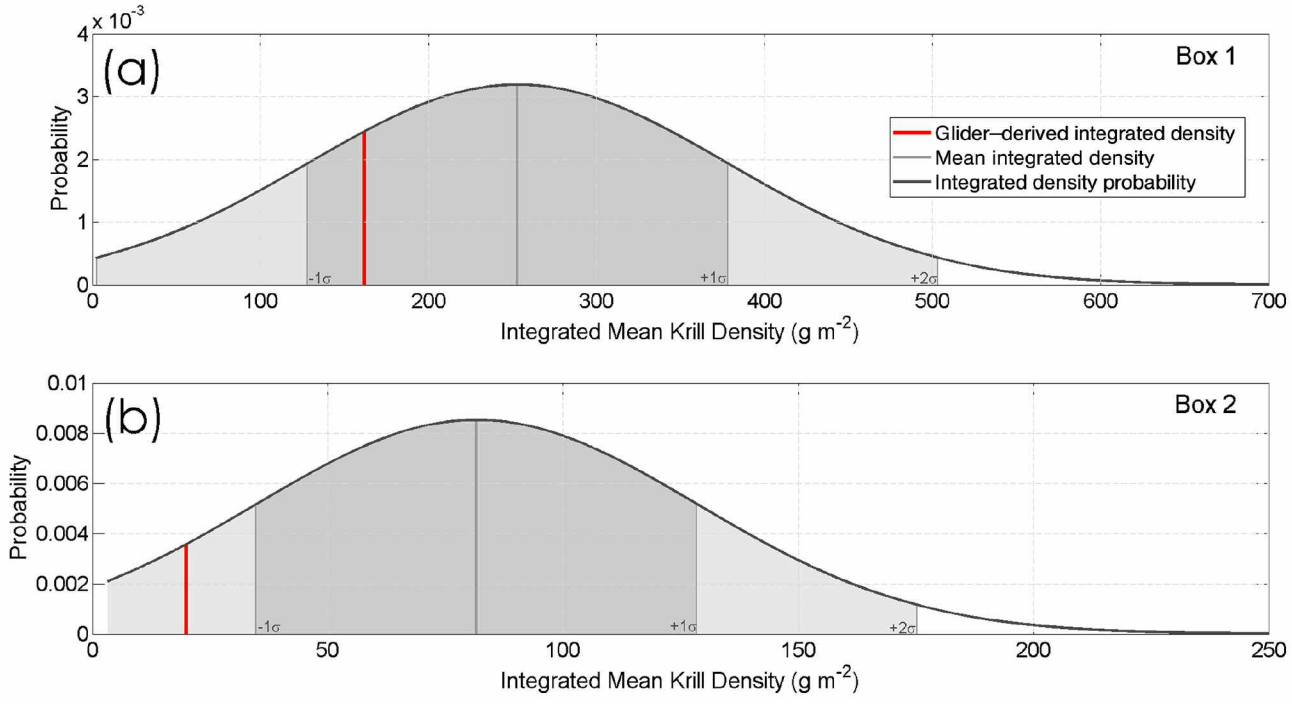

Fig. 9. Probability density functions of the mean integrated krill density estimated from the Monte Carlo simulation of glider-borne ES853 sampling through ship-borne EK60 data for (a) Box 1 and (b) Box 2. The mean integrated density is identified, the dark gray shaded area represents one standard deviation from the mean, and the light gray represents two standard deviations from the mean (95% of the distribution). The observed glider-derived integrated krill density is identified in red.

of glider-borne ES853 sampling through ship-borne EK60 data were undertaken to examine the influence of sampling effort on krill density estimation. Individual dive profile characteristics, from the real glider dive missions (consisting of multiple dives), were applied to randomized start positions within the EK60 120 kHz acoustic data. Conditions of seed placement were the avoidance of both overlapping dives and the geographic truncation of samples by the limits of the EK60 data. An estimate of mean and standard deviation of krill density with depth were derived for each glider mission and krill density was integrated to the common depth of 400 m. The observed glider-derived density in Box 1 was 162.0 g m^{-2}, 65% of the sampling model mean of 247.4 g m^{-2}, but within one standard deviation of the mean of the simulated distribution (Fig. 9a). The observed glider-derived krill density in Box 2 was 20.1 g m^{-2}, 25% of the sample mean (80.8 g m^{-2}) and outside 1 standard deviation from the mean, within the simulated distribution (Fig. 9b). In both cases the observed glider-based mean krill density estimates were within 1 standard deviation of the mean simulated distribution. This suggests that the observed glider-derived profiles were realistic representations of the subsampled EK60 data. The greater deviation from the mean observed in Box 2 may be a function of the large disparity in sampling effort; whereas both boxes share a similar number of glider dives, the corresponding EK60 dataset differs by an order of magnitude in size. It is clear that a greater sampling effort is required to reduce the uncertainty in the density estimate around the mean (i.e., reduce the standard deviation).

To quantify the degree of glider sampling needed for similar confidence between ship and glider surveys of biomass, multiple Monte Carlo simulations (500 iterations, no replacement, seed conditions as above) were undertaken on both boxes, varying the number (n) of dive missions (11 dives) between 1 and 100 (1:10, 12, 14, 16, 18, 20, 25, 30, 40, 50, 75, 100) to represent a greater sampling intensity. Mean krill density profiles were estimated for each iteration and compared with the whole EK60 dataset in the box using a linear regression (R^2). As *n* increases a larger and larger percentage of the whole data set is being sampled, and therefore a greater percentage of the iterations will have an R^2 approaching 1 (Fig. 10a&b). Eighty percent of the modeled dive missions were seen to correlate strongly ($R^2 > 0.9$) with the ship's data in Box 1 when the mission size was 10 times the number of dives actually performed (Figs. 10a&d). In the much larger Box 2, with more EK60 data, the same degree of correlation occurred with 45 times the number of dives actually performed. It is clear from this analysis that a greater number of dives than were achieved are required to appropriately represent the distribution of krill within the surveyed boxes.

Discussion

This article reports the first observations of calibrated, acoustic measurements made from a glider, with a methodology that enables organism density to be estimated, following standard protocols. Two survey boxes were examined and glider-based Antarctic krill density estimates for each box were of the same order of magnitude as those estimated from concurrent ship-based measurements.

Echo integration is the most widely used acoustic method for estimating the abundance of scattering organisms in the sea (Simmonds and MacLennan 2005). Fundamental to this technique is a robust and repeatable measure of energy in echoes received by an echo-sounder, which requires careful calibration of the acoustic instrument (Foote et al. 1987). Whilst acoustic backscatter measurements made from an acoustic Doppler profiler mounted on a glider have shown the relative distribution of whale prey (Baumgartner and Fratantoni 2008), the uncalibrated nature of such an instrument makes robust quantitative measurements unfeasible. Use of acoustic scattering models and a knowledge of taxonomic composition from concurrent net samples have shown a relationship between acoustic Doppler profiler acoustic backscatter and zooplankton (Brierley et al. 1998; Fielding et al. 2004; Ressler and Jochens 2003), though these would be unrepeatable between instruments and over-time without instrument calibration. The ES853 was calibrated using standard on-axis techniques for a single beam echo-sounder (Foote et al. 1987), with a < 1 dB variability in gain over a range of 30-60 m. The change from under- to overestimated gain with depth suggests that measuring the TVG function of the ES853, rather than approximating it with 20log*R*, could further reduce uncertainty of the S_v estimate. In addition, the calibration presented here was undertaken at the sea surface. With the ES853 mounted on a glider that undulates from the surface to 1000 m, the echo-sounder is subjected to large changes in pressure. Kloser (1996) showed that the performance of echo-sounders can vary over depth as a result of deformation of the transducer elements. Further investigation into the performance of the ES853 with depth is required.

The ES853 is a compact and low power echo-sounder, and as such, is constrained in its power and acoustic complexity. This has resulted in a shortened range from the transducer, a limited dynamic range and reduced S_v resolution. To get a good signal-to-noise ratio at a distance from the transducer, there is saturation of the acoustic signal (at 40 dB gain setting) within 24 m of the transducer face at backscattering strengths similar to krill swarms. This reduces the actual usable range of the echo-sounder, although this is offset by the glider diving profiles taking the ES853 through the water column. In turn, however, this may introduce platform avoidance effects (Stoner et al. 2008). Below 20 m no krill swarms were observed at distances of less than 5 m from the glider (e.g., Fig. 6), and swarms often appeared to descend as the glider approached within 15 m. This is contrary to the lack of avoidance of herring to an AUV reported by Fernandes et al. (2000). In their case, the AUV was below the target species, whereas in our scenario the glider is descending on the krill and may appear as the shadow of a predator, such as a seal or penguin. Mounting

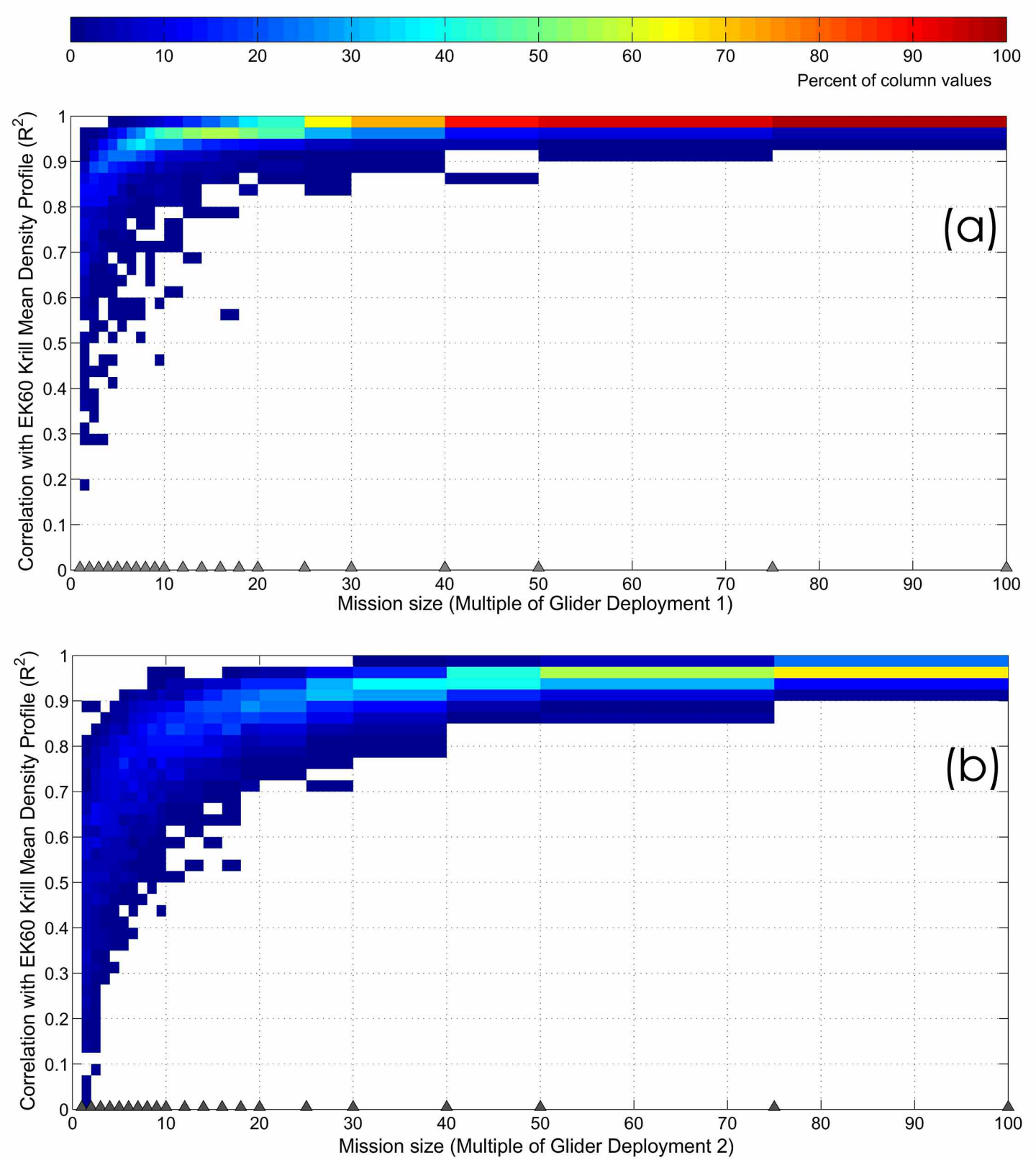

Fig. 10. The percentage (colored blue [~0%] to red [100%]) of correlation (R^2) values between glider-derived ES853 and ship-borne EK60 integrated krill density for (a) Box 1 and (b) Box 2 as the size of the glider mission within the box is increased.

upward and downward looking echo-sounders onto the glider may be particularly informative in resolving platform avoidance behavior, since it is assumed that the glider itself is a quiet platform (Ferguson et al. 2010), with a small visual cross-section and no constantly running machinery that might induce low frequency vibrations. The extent of the stimuli to which marine animals react is still unclear, though it is known that even seemingly minor stimuli can impact behavior (De Robertis and Handegard 2013).

Comments and recommendations

This study shows that it is possible to collect quantitative measurements of acoustic backscatter from zooplankton using an echo-sounder mounted on a glider. We have presented this through an analysis of its use to derive a biomass estimate of Antarctic krill. However, this is not the only application for this sensor. Calibrated acoustic measurements can be used to measure suspended sediment concentration (e.g., Thorne et al. 1991), sea bed type (Orlowski 1984), or bubble (air or oil) presence (Szczucka 1989) that have far wider applications than solely marine ecosystem assessment.

The example presented here of an acoustic assessment of Antarctic krill was undertaken in a region dominated by a single species. Identification of targets within acoustic data typically requires simultaneous multi-frequency measurements (Korneliussen and Ona 2003) and validation through concurrent net or optical sampling (e.g., De Robertis 2001; Lawson et al. 2008). Behavior has also been proposed as a method of identification (Lehodey et al. 2010); here we used clearly identifiable behavior-induced targets (swarms) to identify the species of interest. Ship-borne multi-frequency acoustic measurements and net samples validated this assumption. Target identification remains a key challenge in applying a single frequency echo-sounder to ecosystem assessment. As sensor miniaturization and battery performance increases, greater resolution, improved signal-to-noise ratio and a move to multi-frequency or broadband acoustic measurements from a glider and other AUVs will greatly improve target identification and glider application.

Low-resolution single-frequency acoustic data, even collected at a slow ping interval of 4 s, generates approximately 1 Mb of data over a typical 1000 m glider dive (down and up). Deployment of the glider with an internally logging echo-sounder leaves the mission liable to data loss in the event of glider loss. Presently, the transmission of all the acoustic data by satellite is not feasible due to transmission rates that would require the glider to be at the surface for long periods, therefore at the mercy of strong surface currents, as well as the cost of such high-volume transfer. Key areas for future development in glider and other autonomous systems are improved on-board processing, compression, and transmission of data (Pence et al. 2010). The principal challenge of such work is balancing the computing performance needed to algorithmically analyze volumes of acoustic data, and the power constraints of long-duration platforms. To realize Stommel's vision of a network of intercalibrating gliders with the capacity to dynamically track ocean phenomena (Stommel 1989), such as krill swarms, technological developments in the areas of low-powered processing, battery energy density, and survey detection and decision algorithms are all required.

Glider-derived estimates of krill density in this study reflected those calculated from EK60 data more closely in Box 1 than in Box 2. This was due to the highly variable distribution of the krill swarms, seen as high variability in the mean profiles, along with an order of magnitude greater sample size in the EK60 data of Box 2, compared with Box 1. Note that these were not systematic surveys of the identified boxes, but a comparison of relative sampling effort in the same area. A model of the glider sampling applied to the ship's data suggests a need for 120 dives in Box 1 and 480 dives in Box 2, compared with the 11 and 12 (respectively) that were actually completed in this study, to accurately determine the krill density estimates calculated from the larger amount of ship data. Given the slower travel speed, influence of strong oceanographic currents, more limited range and large vertical movement of the platform, the glider cannot be expected to replicate the acoustic dataset acquired by a vessel in a similar period. There is disproportionally low glider-based acoustic coverage of the near-surface depths, which is particularly relevant when the target species such as krill typically resides in the upper 200 m of the water column. Further development of the glider control parameters, allowing more granular specification of pitch and roll targets, would enable pilots to optimize orientation of the platform during critical phases of a dive. It is recognized, however, that such control would likely incur the cost of reduced fidelity to the intended flight path.

It is important, when using gliders for survey work to consider dive strategies such as shallow (or targeted depth) dives or multiple dives without surfacing as well as extracting usable data from the upcast. Likewise, the directivity and sensitivity of the measurement with respect to the orientation of the platform must be considered. For example, in this case, an additional, upward-facing echo-sounder would effectively double the coverage possible during a glider dive, though would come at the cost of increased power consumption. The use of mechanical stabilization, such as with a gimbal of the echo-sounder is not a satisfactory solution as a glider is typically carefully ballasted and so even subtle changes in the center of gravity of the vehicle can have a large impact on glide angle and dive rate. Technological improvements such as beam steering of a phased array, which would require no moving parts, may increase the amount of useable directional data.

A glider-centric acoustic survey must therefore be flexible in its design. Whereas, with two replicates in this study, it is not reasonable to infer the optimal coverage requirements as a general rule, it is clear that to get appropriate spatial resolution within a short period multiple platforms are required to provide a holistic picture. A combination of platforms with

overlapping sampling strategies is most desirable (Handegard et al. 2012). Notwithstanding the necessity of target identification and TS model parameterization, it is envisaged that a coordinated fleet of acoustic gliders might one day support biomass surveys undertaken by research vessels, extending temporal and spatial coverage by being able to exploit challenging environments such as during winter or during rough weather. It is further possible that such a fleet might, in part, be deployed and serviced from shore or through the use of ships of opportunity, thus reducing the pressure for time aboard research vessels.

Acknowledgments

We are grateful to the masters and crews of the R.R.S. *James Clark Ross* and *Ernest Shackleton* for their support in the deployment and recovery of instruments during JR260b and JR255a. Special thanks are due to Elizabeth Creed for her expert advice and glider piloting, to Imagenex for development of the echo-sounder and to Chris Yahnker for his integration of the echo sounder into the Seaglider. We thank Jon Watkins for his helpful review of the manuscript and the two anonymous reviewers who provided valuable comments. This work was funded by the UK Natural Environment Research Council, Antarctic Funding Initiative grants NE/H014756/1, NE/H01439X/1, and NE/H014217/1, GENTOO Gliders: Excellent New Tools for Observing the Ocean.

References

Asper, V., W. Smith, C. Lee, J. Gobat, K. Heywood, B. Queste, and M. Dinniman. 2011. Using gliders to study a phytoplankton bloom in the Ross Sea, Antarctica, p. 1-7. *In* OCEANS 2011, IEEE, Spain. IEEE Conference Publications.

Atkinson, A., V. Siegel, E. A. Pakhomov, M. J. Jessopp, and V. Loeb. 2009. A re-appraisal of the total biomass and annual production of Antarctic krill. Deep-Sea Res. I 56:727-740 [doi:10.1016/j.dsr.2008.12.007].

Baumgartner, M. F., and D. M. Fratantoni. 2008. Diel periodicity in both sei whale vocalization rates and the vertical migration of their copepod prey observed from ocean gliders. Limnol. Oceanogr. 53:2197-2209 [doi:10.4319/lo.2008.53.5_part_2.2197].

Brierley, A., and others. 2003. An investigation of avoidance by Antarctic krill of RRS James Clark Ross using the Autosub-2 autonomous underwater vehicle. Fish. Res. 60:569-576 [doi:10.1016/S0165-7836(02)00144-3].

Brierley, A. S., M. A. Brandon, and J. L. Watkins. 1998. An assessment of the utility of an acoustic doppler current profiler for biomass estimation. Deep-Sea Res. I 45:1555-1573 [doi:10.1016/S0967-0637(98)00012-0].

———, R. A. Saunders, D. G. Bone, E. J. Murphy, P. Enderlein, S. G. Conti, and D. A. Demer. 2006. Use of moored acoustic instruments to measure short-term variability in abundance of Antarctic krill. Limnol. Oceanogr. Methods 4:18-29 [doi:10.4319/lom.2006.4.18].

Coetzee, J. 2000. Use of a shoal analysis and patch estimation system (SHAPES) to characterise sardine schools. Aquat. Living Resour. 13:1-10 [doi:10.1016/S0990-7440(00)00139-X].

Constable, A. 2001. The ecosystem approach to managing fisheries: Achieving conservation objectives for predators of fished species. CCAMLR Sci. 8:37-64.

Conti, S. G., and D. A. Demer. 2006. Improved parameterization of the SDWBA for estimating krill target strength. ICES J. Mar. Sci. 63(5):928-935 [doi:10.1016/j.icesjms.2006.02.007].

Croxall, J. P., I. Everson, G. L. Kooyman, C. Ricketts, and R. W. Davis. 1985. Fur seal diving behaviour in relation to vertical distribution of krill. J. Anim. Ecol. 55(1):1-8 [doi:10.2307/4616].

———, K. Reid, and P. A. Prince. 1999. Diet, provisioning and productivity responses of marine predators to differences in availability of Antarctic krill. Mar. Ecol. Prog. Ser. 177:115-131 [doi:10.3354/meps177115].

Dassatti, A., M. van der Schaar, P. Guerrini, S. Zaugg, L. Houegnigan, A. Maguer, and M. Andre. 2011. On-board underwater glider real-time acoustic environment sensing, p. 1-8. *In* OCEANS 2011, IEEE, Spain. IEEE Conference Publications.

Davis, R. E., M. D. Ohman, D. L. Rudnick, and J. T. Sherman. 2008. Glider surveillance of physics and biology in the southern California Current System. Limnol. Oceanogr. 53:2151-2168 [doi:10.4319/lo.2008.53.5_part_2.2151].

De Robertis, A. 2001. Validation of acoustic echo counting for studies of zooplankton behavior. ICES J. Mar. Sci. 58(3):543-561 [doi:10.1006/jmsc.2000.1059].

———, and N. O. Handegard. 2013. Fish avoidance of research vessels and the efficacy of noise-reduced vessels: a review. J. Mar. Sci. 70(1):34-45.

Demer, D. A., and S. G. Conti. 2005. New target-strength model indicates more krill in the Southern Ocean. ICES J. Mar. Sci. 62:25-32 [doi:10.1016/j.icesjms.2004.07.027].

Dunford, A. J. 2005. Correcting echo-integration data for transducer motion. J. Acoust. Soc. Am. 118(4):2121-2123 [doi:10.1121/1.2005927].

Eriksen, C., and others. 2001. Seaglider: a long-range autonomous underwater vehicle for oceanographic research. IEEE J. Ocean. Eng. 26:424-436 [doi:10.1109/48.972073].

Ferguson, B. G., K. W. Lo, and J. D. Rodgers. 2010. Sensing the underwater acoustic environment with a single hydrophone onboard an undersea glider, p. 1-5. *In* OCEANS 2010, IEEE, Sydney. IEEE Conference Publications.

Fernandes, P. G., A. S. Brierley, E. J. Simmonds, and N. W. Millard. 2000. Fish do not avoid survey vessels. Nature 404:35-36 [doi:10.1038/35003648].

———, P. Stevenson, A. S. Brierley, F. Armstrong, and E. J. Simmonds. 2003. Autonomous underwater vehicles: future platforms for fisheries acoustics. ICES J. Mar. Sci. 60:684-691 [doi:10.1016/S1054-3139(03)00038-9].

Fielding, S., G. Griffiths, and H. S. J. Roe. 2004. The biological

validation of ADCP acoustic backscatter through direct comparison with net samples and model predictions based on acoustic-scattering models. ICES J. Mar. Sci. 61:184-200 [doi:10.1016/j.icesjms.2003.10.011].

———, and others. 2011. The ASAM 2010 assessment of krill biomass for area 48 from the Scotia Sea CCAMLR 2000 synoptic survey. CCAMLR document WG-EMM 11/20. CCAMLR.

———, J. Watkins, M. Collins, P. Enderlein, and H. J. Venables. 2012. Acoustic determination of the distribution of fish and krill across the Scotia Sea in spring 2006, summer 2008, and autumn 2009. Deep Sea Res. II. 59-60:173-188 [doi:10.1016/j.dsr2.2011.08.002].

———, and others. In press. Inter-annual variability in Antarctic krill (*Euphausia superba*) density at South Georgia, Southern Ocean: 1997-2013. ICES J. Mar. Sci.

Foote, K., H. Knudsen, G. Vestnes, D. N. Maclennan, and E. J. Simmonds. 1987. Calibration of acoustic instruments for fish density estimation: A practical guide. ICES Coop. Res. Rep. 144:69.

Griffiths, G., and others. 2001. Standard and special: Sensors used during the Autosub Science Missions programme. Proc. AUSI Sensors Workshop, Miami. <http://archive.auvac.org/research/publications/files/2001/Autosub_AUSI_Sensors_paper.pdf>

Handegard, N. O., and others. 2012. Towards an acoustic-based coupled observation and modelling system for monitoring and predicting ecosystem dynamics of the open ocean. Fish Fisher. 14:605-615 [doi:10.1111/j.1467-2979.2012.00480.x].

Hewitt, R. P., and others. 2004. Biomass of Antarctic krill in the Scotia Sea in January/February 2000 and its use in revising an estimate of precautionary yield. Deep Sea Res. II 51:1215-1236 [doi:10.1016/j.dsr2.2004.06.011].

Johnson, K. S., and others. 2009. Observing biogeochemical cycles at global scales with profiling floats and gliders: Prospects for a global array. Oceanography 22:216-225 [doi:10.5670/oceanog.2009.81].

Klinck, H., and others. 2012. Near-real-time acoustic monitoring of beaked whales and other cetaceans using a seaglider. PLoL One 7(5) [doi:10.1371/journal.pone.0036128].

Kloser, R. J. 1996. Improved precision of acoustic surveys of benthopelagic fish by means of a deep-towed transducer. ICES J. Mar. Sci. 53:407-413 [doi:10.1006/jmsc.1996.0057].

Korneliussen, R. J., and E. Ona. 2003. Synthetic echograms generated from the relative frequency response. ICES J. Mar. Sci. 60:636-640 [doi:10.1016/S1054-3139(03)00035-3].

Lawson, G., P. Wiebe, and T. Stanton. 2008. Euphausiid distribution along the Western Antarctic Peninsula—Part A: Development of robust multi-frequency acoustic techniques to identify euphausiid aggregations and quantify euphausiid size, abundance, and biomass. Deep-Sea Res. II 55:412-431 [doi:10.1016/j.dsr2.2007.11.010].

Lehodey, P., R. Murtugudde, and I. Senina. 2010. Bridging the gap from ocean models to population dynamics of large marine predators: A model of mid-trophic functional groups. Prog. Oceanogr. 84(1):69-84 [doi:10.1016/j.pocean.2009.09.008].

Lubchenco, J., and others. 1991. The sustainable biosphere initiative—an ecological research agenda. Ecol. 72(2):371-412 [doi:10.2307/2937183].

McGehee, D., R. O'Driscoll, and L. V. Martin Traykovski. 1998. Effects of orientation on acoustic scattering from Antarctic krill at 120 kHz. Deep-Sea Res. II. 45:1273-1294 [doi:10.1016/S0967-0645(98)00036-8].

Medwin, H., and C. S. Clay. 1998. Fundamentals of acoustical oceanography. Academic Press.

Morris, D. J., J. L. Watkins, C. Ricketts, F. Buchholz, and J. Priddle. 1988. An assessment of the merits of length and weight measurements of Antarctic krill *Euphausia superba*. Bull. Br. Antarct. Surv. Bull. 79:27–50.

Murphy, E. J., and others. 2007. Spatial and temporal operation of the Scotia Sea ecosystem: a review of large-scale links in a krill centred food web. Phil. Trans. R. Soc. B. 362(1477):113-148.

Nicol, S., and Y. Endo. 1999. Krill fisheries: Development, management and ecosystem implications. Aquat. Living Resour. 12(2):105-120 [doi:10.1016/S0990-7440(99)80020-5].

Orlowski, A. O. 1984. Application of multiple echoes energy measurement for evaluation of sea bottom type. Oceanologica 19:61-78.

Osse, T. J., and C. C. Eriksen. 2007. The Deepglider: A full ocean depth glider for oceanographic research, p. 1-12. *In* OCEANS 2007, IEEE, Vancouver. IEEE Conference Publications.

Pence, W. D., R. L. White, and R. Seaman. 2010. Optimal compression of floating-point astronomical images without significant loss of information. Pub. Astronom. Soc. Pac. 122(895):1065-1076 [doi:10.1086/656249].

Perry, M. J., B. S. Sackmann, C. C. Eriksen, and C. M. Lee. 2008. Seaglider observations of blooms and subsurface chlorophyll maxima off the Washington coast. Limnol. Oceanogr. 53(5, part 2):2169-2179 [doi:10.4319/lo.2008.53.5_part_2.2169].

Queste, B. Y., and others. 2012. Deployments in extreme conditions: Pushing the boundaries of Seaglider capabilities, p. 1-7. Proc. 2012 IEEE/OES Autonomous Underwater Vehicles (AUV). IEEE.

Reid, K., J. L. Watkins, E. J. Murphy, P. N. Trathan, S. Fielding, and P. Enderlein. 2010. Krill population dynamics at South Georgia: implications for ecosystem-based fisheries management. Mar. Ecol. Prog. Ser. 399:243-252 [doi:10.3354/meps08356].

Reiss, C. S., A. M. Cossio, V. Loeb, and D. A. Demer. 2008. Variations in the biomass of Antarctic krill (*Euphausia superba*) around the South Shetland Islands, 1996-2006. ICES J. Mar. Sci. 65:497-508 [doi:10.1093/icesjms/fsn033].

Ressler, P. H., and A. E. Jochens. 2003. Hydrographic and

acoustic evidence for enhanced plankton stocks in a small cyclone in the northeastern Gulf of Mexico. Cont. Shelf Res. 23(1):41-61 [doi:10.1016/S0278-4343(02)00149-8].

Roe, H. S. J., and D. M. Shale. 1979. A new multiple rectangular midwater trawl (RMT 1+8M) and some modifications to the institute of oceanographic sciences' RMT 1+8. Mar. Biol. 50:283-288 [doi:10.1007/BF00394210].

SC-CCAMLR. 2010. Report of the Twenty-ninth Meeting of the Scientific Committee (SC-CCAMLR-XXIX). CCAMLR.

Schmidt, K., and others. 2011. Seabed foraging by Antarctic krill: implications for stock assessment, bentho-pelagic coupling and the vertical transfer of iron. Limnol. Oceanogr. 56(4):1411-1428 [doi:10.4319/lo.2011.56.4.1411].

Sherman, J., R. E. Davis, W. B. Owens, and J. Valdes. 2001. The autonomous underwater glider "spray." IEEE J. Oceanic Eng. 26(4):437-446 [doi:10.1109/48.972076].

Shulman, I., and others. 2009. Impact of glider data assimilation on the Monterey Bay model. Deep Sea Res. I. 56:188-198 [doi:10.1016/j.dsr2.2008.08.003].

Simmonds, E. J., and D. N. MacLennan. 2005. Fisheries acoustics: Theory and practice, 2nd ed. Oxford: Blackwell Science [doi:10.1002/9780470995303].

Stommel, H. 1989. The Slocum mission. Oceanography 2(1):22-25 [doi:10.5670/oceanog.1989.26].

Stoner, A. W., C. H. Ryer, S. J. Parker, P. J. Auster, and W. W. Wakefield. 2008. Evaluating the role of fish behavior in surveys conducted with underwater vehicles. Can. J. Fish. Aquat. Sci. 65(6):1230-1243 [doi:10.1139/F08-032].

Szczucka, J. 1989. Acoustic detection of gas bubbles in the sea. Oceanologia 28:103-114

Tarling, G. A., and others. 2009. Variability and predictability of Antarctic krill swarm structure. Deep Sea Res. I 56:1994-2012 [doi:10.1016/j.dsr.2009.07.004].

Thorne, P. D., C. E. Vincent, P. J. Hardcastle, S. Rehman, and N. Pearson. 1991. Measuring suspended sediment concentrations using acoustic backscatter devices. Mar. Geol. 98 (1):7-16 [doi:10.1016/0025-3227(91)90031-X].

Ullgren, J. E., and M. White. 2010. Water mass interaction at intermediate depths in the southern Rockall Trough, northeastern North Atlantic. Deep-Sea Res. I. 57(2):248-257 [doi:10.1016/j.dsr.2009.11.005].

Urick, R. J. 1983. Principles of underwater sound, 3rd ed. McGraw-Hill.

Watkins, J. L., and A. S. Brierley. 1996. A post-processing technique to remove background noise from echo integration data. ICES J. Mar. Sci. 53:339-344 [doi:10.1006/jmsc.1996.0046].

———, R. Hewitt, M. Naganobu, and V. Sushin. 2004. The CCAMLR 2000 Survey: a multinational, multi-ship biological oceanography survey of the Atlantic sector of the Southern Ocean. Deep-Sea Res. II. 51:1205-1213 [doi:10.1016/j.dsr2.2004.06.010].

Webb, D. C., P. J. Simonetti, and C. P. Jones. 2001. SLOCUM: an underwater glider propelled by environmental energy. IEEE J. Oceanic Eng. 26:447-452 [doi:10.1109/48.972077].

Yahnker, C., E. Creed, K. J. Heywood. 2012. iRobot Seaglider With Ogive Fairings Supports Antarctic Research: Increased payload capacity from ogive fairings enables AUV to track krill biomass distribution in Weddell Sea. Sea Technology 53(7):10-13.

Submitted 3 December 2013
Revised 9 May 2014
Accepted 23 May 2014